Construction and Building Materials 376 (2023) 131051

Contents lists available at ScienceDirect

Construction and Building Materials

journal homepage: www.elsevier.com/locate/conbuildmat

Biochar and recycled carbon fibres as additions for low-resistive cement-based composites exposed to accelerated degradation

A. Mobili [a], G. Cosoli [b,*], N. Giulietti [c], P. Chiariotti [c], T. Bellezze [a], G. Pandarese [b], G.M. Revel [b], F. Tittarelli [a,d]

[a] Department of Materials, Environmental Sciences and Urban Planning (SIMAU), Università Politecnica delle Marche – INSTM Research Unit, 60131 Ancona, Italy
[b] Department of Industrial Engineering and Mathematical Science (DIISM), Università Politecnica delle Marche, 60131 Ancona, Italy
[c] Department of Mechanical Engineering, Politecnico di Milano, 20156 Milano, Italy
[d] Institute of Atmospheric Sciences and Climate, National Research Council (ISAC-CNR), Via Gobetti 101, 40129 Bologna, Italy

ARTICLE INFO

Keywords:
Concrete
Carbon-based additions
Biochar
Carbon fibres
Electrical impedance measurement
Capillary water absorption
Chloride penetration
Carbonation
Durability

ABSTRACT

Biochar (BCH) and recycled carbon fibres (RCF) were used as carbonaceous additions in low-resistive mortars/concretes. Their effects on mechanical, electrical, and durability properties were investigated. Tests were performed both during curing and accelerated degradation. The combined use of RCF and BCH decreased the electrical impedance of cement-based matrices, enabling the use of low-cost monitoring instrumentation, and improved their mechanical performance. Recycled carbon fibres and biochar additions increased carbonation and capillary water absorption but acting as a barrier they made water and chlorides penetrate less deeply.

1. Introduction

Conductive fibres and fillers based on carbon are often added in concrete to enhance self-sensing and electromagnetic shielding properties, to reinforce the material, and to improve thermal and acoustic properties [1]. The present authors have previously tested both recycled carbon fibres (RCF) and gasification char (GCH) as additions in pastes, mortars, and concretes [2] to increase both electrical conductivity and mechanical strength. The current European regulations allow the use of the tested GCH (CER Code 100103) in mortars/concretes. However, safety issues can be raised owing to its high content of aromatics (benzene 308 mg/kg, toluene 93 mg/kg, ethylbenzene 16 mg/kg, xylene 8 mg/kg, and ethyltoluene 2 mg/kg, for a total of 428 mg/kg tested according to the DIN ISO 22155–05 standard), which prevent its use in some European countries, where local regulations are more restrictive than the European ones. Therefore, the authors looked for an alternative material, namely biochar (BCH). Biochar is a by-product obtained from the pyrolysis of different types of vegetable biomass, including forestry and agricultural residues, to obtain a gas (syngas) with a calorific value equal to liquefied petroleum gas (LPG), which can be used in production processes. Biochar was chosen as alternative to gasification char because of multiple reasons: i) BCH has a lower aromatics content than GCH (benzene 1.0 mg/kg, toluene 1.3 mg/kg, ethylbenzene 0.1 mg/kg, xylene 0.4 mg/kg, and ethyltoluene < 0.1 mg/kg, for a total of 3 mg/kg tested according to the DIN ISO 22155–05 standard); ii) BCH structure seems to be similar to GCH, being a by-product produced by the thermal treatment (pyrolysis) of biomass and other organic matter [3], thus also its physical, mechanical, and electrical properties might be comparable; iii) the availability of BCH is high due to the wide diffusion of thermal biomass power plants. Moreover, BCH is rich in carbon and has a microporous structure making it useful for different applications, such as soil quality enhancement, removal of heavy metals from aqueous solutions, and as fuel [4]. It can be stated that including biochar in concrete improves both mechanical strength (the optimum content is of approximately 2 wt% [5]) and thermal properties. Indeed, it is able to effectively replace part of cement, contributing to reduce CO_2 emissions [6]. Furthermore, biochar is being investigated also to obtain carbon–neutral concrete, thanks to its capability of storing CO_2 absorbed from atmosphere [7]. Gupta et al. [8] highlighted the improved water tightness and mechanical performance of concrete thanks to BCH addition.

* Corresponding author.
E-mail address: g.cosoli@staff.univpm.it (G. Cosoli).

https://doi.org/10.1016/j.conbuildmat.2023.131051
Received 30 December 2022; Received in revised form 10 March 2023; Accepted 12 March 2023
Available online 20 March 2023
0950-0618/© 2023 The Authors. Published by Elsevier Ltd. This is an open access article under the CC BY license (http://creativecommons.org/licenses/by/4.0/).

They reported that an addition of BCH at 0.5 wt% offers an improvement of 16% in compressive strength at 28 days, whereas an addition at 1.0 wt % reduces capillary water absorption and water penetration depth by 28% and 43%, respectively. The improvement in terms of compressive strength is confirmed by other studies. Akhtar and Sarmah reported that an addition of BCH at 0.1 vol% in concrete increases compressive strength of approximately 20%, without significantly modifying water absorption [9]. Gupta and Kua [10] observed an enhanced mechanical performance (40–50% in terms of compressive strength) with the addition of pre-soaked biochar at 2.0 wt%. Biochar also increases the water retention capability, the hydration degree, and the water tightness by reducing the water accessible porosity (18–20%) and the water penetration depth (55–60%). The increased water retention capability due to biochar addition is highlighted also by Choi et al. [11], who reported that more water is required in the mix-design when biochar is added owing to its carbon content and particular porous microstructure. Several other applications have been investigated in the literature. Zao et al. [12] investigated the use of BCH in vegetation concrete, finding that a content of 5 kg/m^3 is optimal for ryegrass growth, thanks to its large surface area and microstructure enhancing water retention capacity. Cuthbertson et al. [13] used BCH as a filler to improve thermal and acoustic properties of concrete. They noticed that an increased BCH content (maximum 12 wt% to preserve concrete integrity) leads to reduced density and provides better sound absorption and thermal insulation properties. Gupta et al. [14] discussed about the possibility of using BCH in construction materials to capture and lock atmospheric CO_2, thus contributing to reduce greenhouse gases emissions. Kua et al. [15] investigated the employment of BCH as a carrier for bacteria spores in concrete aimed to decrease permeability and recover sorptivity after loading cycles (causing damages and cracks). This contributes to reduce repair costs and extend the service life of concrete buildings. Falliano et al. [16] found that the addition of BCH at 2.0 wt% (mixed with cement in dry status) improves the fracture behaviour of foamed concrete, without impairing the flexural strength. The positive effect of biochar on cracking (e.g., post-cracking ductility and early-shrinkage cracking) is confirmed by other studies [17,18].

On the other hand, carbon fibres have been extensively used to cast self-sensing and low-resistive concretes, since they are extremely suitable to enable the monitoring of the compressive strain of concrete elements thanks to their physical and chemical properties [19]. According to Belli et al. [20], an addition of 0.1 vol% of virgin carbon fibres (VCF) is able to decrease of more than 10% the electrical resistivity of cement mortars, whereas 0.05 vol% of recycled carbon fibres (RCF) decreases electrical resistivity of even 70%. However, an addition higher than 1.2 vol% of VCF or RCF causes a decrease of compressive strength because of the presence of voids produced by fibre clumps, although the flexural and tensile strengths continue to increase until dosages equal to 1.6 vol %. Moreover, the use of RCF instead of VCF is attracting a wider and wider attention for the circular economy principles focused to reduce the concrete environmental impact [21]; the RCF diffusion is growing, with an expected market of 222 million USD by 2026 (with a compound annual growth rate of 12%) [22]. The present authors have already tested RCF in concrete, finding that their addition at 0.05 vol% on the total provides a decrease of electrical impedance equal to 6%. This decrease significantly enhances (74%) when used in combination with gasification char at 1.0 vol% on the total [23].

Even if the literature on the use of carbon-based additions to manufacture multifunctional mortars/concretes is already wide, according to the best of the authors' knowledge, there are no studies reporting the combined use of two carbon-based by-products as RCF and BCH. Therefore, the aim of this study is to evaluate the performance of BCH used in substitution of GCH as a conductive filler in cement-based mortars/concretes. At first, five different types of BCH have been tested in cement mortars to evaluate their effects on mechanical and electrical properties. Then, the best performing BCH has been selected and added to concretes with/without RCF to investigate their effect on the mechanical, electrical, and durability properties. These additions have been chosen for their low cost and sustainability [20,24], besides giving promising mechanical and electrical properties. Since the building material sector represents 10% of CO_2 emissions and approximately 85% of these emissions are linked to cement production [25], a low-clinker cement, developed within the EnDurCrete project (GA No. 760639), was used. The different concrete compositions have been characterized in terms of mechanical performance (compressive and tensile strength) and electrical impedance (the Wenner's method was applied, using stainless-steel electrodes installed in concrete specimens during the casting phase). Since concrete durability (i.e., its capability to withstand deterioration processes [26]) is directly related to the exposure environment [27], the specimens have been exposed to five different aggressive environments for accelerated degradation tests: salt-spray chamber, accelerated carbonation, capillary water absorption, and wet/dry cycles in water and in a chloride-rich solution. All these aspects can be monitored through electrical impedance measurements, which could be adopted as a long-term monitoring technique. Indeed, the use of conductive additions in mortars/concretes decreases their electrical resistivity, enabling to perform long-term monitoring with low-cost instrumentation. Since aggressive agents penetrating in mortar/concrete matrices are often represented by water and ions, affecting their electrical impedance [28,29], the existence of a correlation between the measured electrical impedance of concrete and its degradation status has already been stressed [23]. Therefore, this monitoring strategy can early detect the contaminants ingress, facilitating to act promptly and avoid a possible premature failure of the structure.

2. Materials

2.1. Biochar types

Biochar is typically commercialized in pellet form (Fig. 1a). However, before being added into mortars/concretes, it should be ground to maximize its dispersion and optimize its effect on concrete electrical resistivity [30,31]. For this reason, BCH was ground and sieved at a particle size lower than 75 μm (Fig. 1b).

Five different types of BCH were tested before choosing the one to be added into the final concrete mixes:

- FC: Filtercarb Biochar (supplied by Carbonitalia) is a vegetal granular coal not activated with chemicals and obtained through the carbonization process at 700 °C of wood not chemically treated after abatement;
- RAV: this biochar (supplied by RES Italia) is a vegetal granular coal obtained by the pyrolysis of agricultural wastes at 850 °C;
- WSP: this biochar (supplied by UK Biochar Research Centre) is obtained by Wheat Straw Pellets and is produced in a pilot-scale rotary kiln pyrolysis unit with a nominal peak temperature of 700 °C;
- OSR: this biochar (supplied by UK Biochar Research Centre) is obtained by Oil Seed Rape Straw Pellets and is produced in a pilot-scale rotary kiln pyrolysis unit with a nominal peak temperature of 550 °C;
- RH: this biochar (supplied by UK Biochar Research Centre) is obtained by Rice Husk and is produced in a pilot-scale rotary kiln pyrolysis unit with a nominal peak temperature of 550 °C.

For comparison, the authors tested again the GCH, obtained by the gasification of wood chips by means of a Holz-Kraft, Spanner Re^2 GmbH gasifier [2] used in previous experiments. Gasification char was also ground and sieved at 75 μm.

2.2. Mortar specimens

Mortar specimens were cast with a limestone cement CEM II A-LL 42.5 R; a calcareous sand (0/8 mm) was used in saturated surface dry (s.s.d.) condition (water absorption of 2 wt%). An acrylic-based

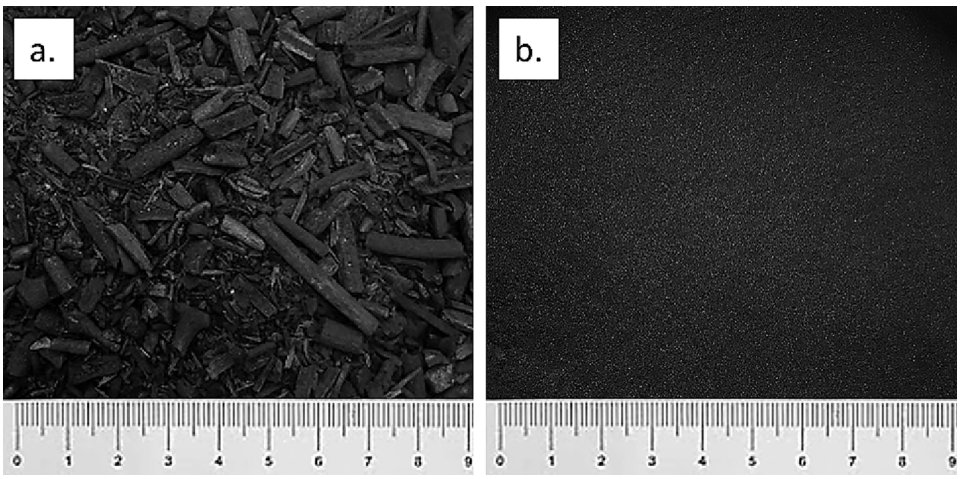

Fig. 1. a. Biochar in pellet form and b. ground and sieved biochar (particle size < 75 μm). Measurements are in cm.

superplasticizer (Dynamon SP1, Mapei S.p.A.) was used as admixture to manufacture mortars with the same workability class (plastic, with a flow value between 140 and 210 mm according to the EN 1015:3 standard), with a water/cement (w/c) ratio equal to 0.50 and a sand/cement (s/c) ratio equal to 3. Both GCH and all the different types of BCH were added at 0.5 vol% on the total. A reference mortar (mREF) without GCH/BCH addition was also manufactured. The mix design of mortars is as follows:

- mREF was manufactured with 510 kg/m^3 of cement, 255 kg/m^3 of water, 1530 kg/m^3 of sand and 2.79 kg/m^3 of Dynamon SP1;
- mortars containing char/biochar were manufactured with 508 kg/m^3 of cement, 254 kg/m^3 of water, 1523 kg/m^3 of sand, 2.78 kg/m^3 of Dynamon SP1 and 10.2 kg/m^3 of char/biochar.

The mortar batches were mixed in a mortar mixer, by adding at first powder materials (sand, GCH/BCH, and cement) and mixed for 2 min. Then, water and subsequently superplasticizer were added and mixed for 3 and 10 min, respectively.

The mixture was poured in different moulds depending on the tests to be carried out on specimens: specimens with 4 cm × 4 cm × 16 cm dimensions were used for compressive strength tests, whereas for electrical impedance tests mortar specimens were equipped with 4 stainless-steel rods to be used as electrodes. In particular, Ø3 mm and 4 cm long rods were embedded for half of their length with a distance of 2 cm, as reported in Fig. 2.

Mortar specimens were cured in a climatic chamber at a temperature (T) of 20 ± 1 °C and a relative humidity (RH) of 95 ± 5% for 7 days, by wrapping them in polyethylene films. Then, plastic films were removed and specimens were left in a climatic chamber (i.e., T = 20 ± 1 °C and RH = 50 ± 5%) until testing.

2.3. Concrete specimens

Concrete specimens were manufactured with a new cement, CEM II/C-M (S-LL), developed by HeidelbergCement AG within the frame of EnDurCrete project [32], whose composition is reported in Table 1. It is a blend of ordinary Portland cement (OPC), ground granulated blast furnace slag (GGBFS), and limestone filler. Being manufactured with only 50 wt% of OPC, in 2021 this low-clinker cement has been added by the European Standardization Committee to the family of common cements within the scope of the European standard EN 197–1. The complete description and characteristics of this cement are reported in a separate paper [33].

Calcareous sand (0/4 mm) was used as fine aggregate, whereas intermediate (5/10 mm) and coarse (10/15 mm) river gravels were used as coarse aggregates. Aggregates, supplied by Nuova Tesi System Srl, have water absorption of 0.4%, 0.9%, and 0.7%, respectively, and their particle size distribution is reported in Fig. 3.

As conductive carbon-based additions, 6 mm-long recycled carbon fibres CGF-6 supplied by Procotex Belgium SA (Fig. 4) and BCH (Fig. 1b) were used. Recycled carbon fibres are a mix of carbon and graphite polyacrylonitrile fibres obtained by polyacrylonitrile precursor, which

Table 1
Composition [wt%] of CEM II/C-M (S-LL) cement.

Cement	OPC	GGBFS	Limestone filler
CEM II/C-M (S-LL)	50	40	10

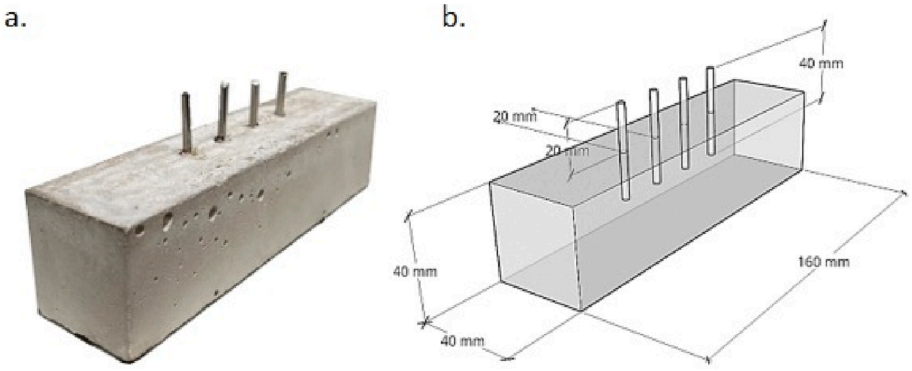

Fig. 2. Configuration of electrodes for electrical impedance measurements in mortars specimens: a. picture and b. drawing with dimensions.

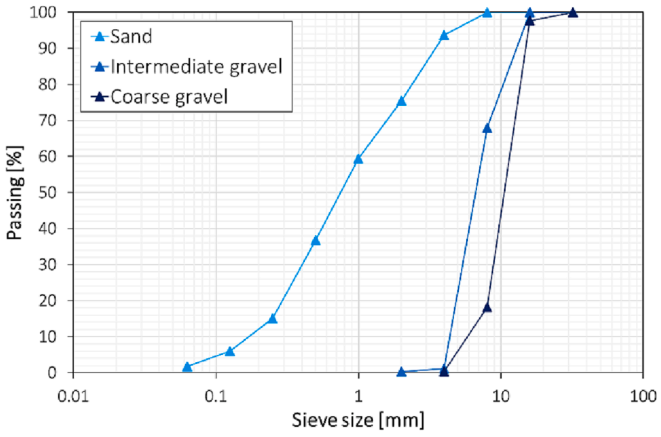

Fig. 3. Particle size distribution of aggregates.

Fig. 4. Recycled carbon fibres.

come from spools of pure carbon fibres [20]. The BCH used in concretes mixes was the one which has given to mortars the best compromise between mechanical and electrical properties, hence high compressive strength and low electrical impedance value (see Section 4.1). The specific surface area is equal to 46.2 m^2/g and 0.132 m^2/g for BCH and RCF, respectively. The average density is equal to 2.00 g/cm^3 and 1.85 g/cm^3 for BCH and RCF, respectively. Concerning the chemical composition, biochar is 100% amorphous carbon, whereas recycled carbon fibres have a carbon content of 94%. Biochar and recycled carbon fibres were added at 0.5 vol% and 0.05 vol% on the total, respectively.

Two polycarboxylate (PC)-based admixtures supplied by Sika AG were used to manufacture concretes with the same workability (S5 class), with a w/c ratio equal to 0.42. In particular, PC2 is a high-water reducing admixture and PC3 is a slump keeper.

The effect of conductive additions was evaluated in four different concrete compositions: 1) REF EDC is the reference concrete without any additions, 2) RCF EDC is the concrete with the addition of RCF at 0.05 vol% on the total, 3) BCH EDC is the concrete with the addition of BCH at 0.5 vol% on the total, 4) RCF + BCH EDC is the concrete with the addition of both RCF at 0.05 vol% and BCH at 0.5 vol% on the total. In concrete mixtures containing carbon-based additions, it was necessary to increase the admixtures dosage to reach the same workability class of concretes, probably because of the high specific surface of RCF and BCH. The mix-design of the four compositions is reported in Table 2.

The concrete batches were mixed in a concrete mixer, by adding at first dry materials (aggregates, BCH, RCF, and cement) and mixing for 5 min. Then, water was added and mixed for 5 min; finally, PC2 and PC3 were incorporated and dosed to reach S5 workability class and mixed for 20 min. Concrete was poured in different moulds depending on the following tests to carry out on specimens: cubes of 10 cm per side and parallelepiped moulds (10 cm × 10 cm × 20 cm) for mechanical tests. Parallelepiped specimens were provided with 4 stainless-steel rods to be used as electrodes for electrical impedance measurements. Rods with a diameter of 3 mm and 4 cm long were embedded for half of their length, as reported in Fig. 5; the inter-electrode spacing was equal to 40 mm.

Concrete specimens were cured in a climatic chamber at T = 20 ± 1 °C and RH > 95% for 28 days by wrapping them in polyethylene films. Then, plastic films were removed and specimens were left at room conditions (i.e., T = 20 ± 5 °C and RH = 50 ± 5%) before testing. Accelerated degradation tests were started after a total of 35 days from the casting day.

3. Methods

3.1. Mechanical tests

To evaluate the mechanical performance of mortars, their compressive strength (R_c) was measured on 4 cm × 4 cm × 16 cm specimens after 1, 7, and 35 days of curing, according to the EN 1015–11 standard. Three specimens per mixture were tested and the average result reported. For concrete mixes, their R_c was measured in compliance to the standard EN 12390–3 at 1, 7, and 28 days after cast on three cubic specimens (10 cm per side) and the average result is reported for each test time. After 28 days of curing, also tensile splitting strength test was carried out on three cubic specimens (10 cm per side) according to the EN 12390–6 standard.

3.2. Electrical impedance measurements

The electrical impedance of mortars/concretes was measured according to the Wenner's method [34]. Alternating Current (AC) measurement was carried out at 10 kHz, by exciting the material through an electric current injected through the external electrodes (i.e., Working Electrode, WE, and Counter Electrode, CE) and measuring the corresponding potential difference between the internal ones (i.e., Sensing, S, and Reference Electrode, RE). Galvanostatic mode of Gamry Reference 600 Potentiostat/Galvanostat was used to carry out the measurements. Results are reported only in terms of the real part of impedance, which is the most affected by concrete durability [35]. Electrical impedance was measured both during curing and accelerated degradation tests. After 28 days of curing, five different durability tests were performed: capillary water absorption, salt-spray chamber exposure, accelerated carbonation, water penetration (wet/dry cycles), and chloride penetration (wet/dry cycles). For the entire duration of testing, concrete specimens (one per composition) dedicated to monitor the effect of simple curing on electrical impedance (curing monitoring) were also considered (except for those exposed to wet/dry cycles). In this way, during exposure tests the contribution of degradation and the contribution of curing on the variation of electrical impedance value can be identified.

3.3. Accelerated carbonation and phenolphthalein tests

Concrete specimens were kept inside a CO_2 chamber at T = 21 ± 1 °C, RH = 60 ± 10%, CO_2 = 3 ± 0.2 vol%. The measurements included both electrical impedance and carbonation depth assessment and were carried out at 0 (i.e., start of test, after 35 days of curing), 7, 14, and 21

Table 2
Mix-design of concrete specimens.

Mixture	Cement [kg/m^3]	Water [kg/m^3]	Sand [kg/m^3]	Intermediate gravel [kg/m^3]	Coarse gravel [kg/m^3]	Air [%]	Admixture [kg/m^3] PC2	PC3	BCH [kg/m^3]	RCF [kg/m^3]
REF EDC	375	158	912	366	623	2.4	1.10	1.27	–	–
RCF EDC	375	158	911	365	622	2.4	1.46	1.42	–	0.92
BCH EDC	373	157	907	363	619	2.4	1.45	1.41	10.20	–
BCH + RCF EDC	373	157	907	363	619	2.4	1.45	1.41	10.20	0.92

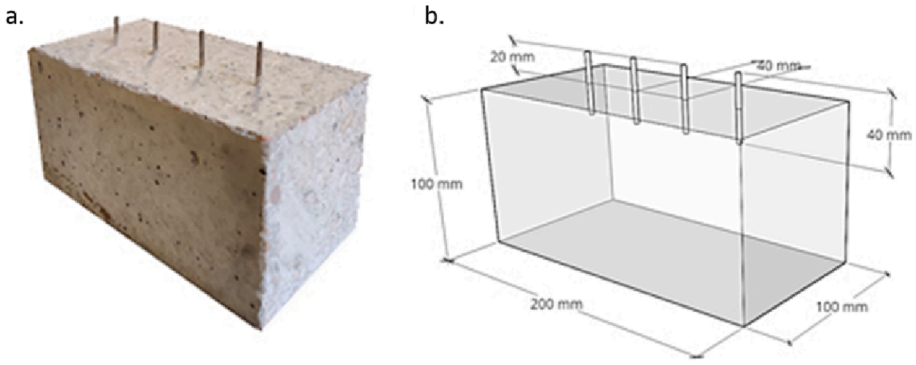

Fig. 5. Configuration of electrodes for electrical impedance measurements in concrete specimens: a. picture and b. drawing with dimensions.

days of exposure. Phenolphthalein test was carried out to measure carbonation depth in compliance with the standard EN 13295 [36] on dedicated specimens with the same compositions and the same exposure conditions of specimens for electrical impedance measurements. An automated system for the objective and accurate measurement of the carbonation depth, previously developed by the present authors, was used [37]. In brief, specimens were broken and the internal surface was treated with 1% solution of phenolphthalein in alcohol. In this way, purple-red colouration was obtained where carbonation had not occurred; otherwise, concrete remained uncoloured. The developed system allowed to frame an image of the test surface and to automatically examine it, thus providing mean and maximum carbonation depth values.

3.4. Exposure to salt-spray chamber

Salt-spray chamber test was carried out according to the UNI EN ISO 9227 standard. Concrete specimens were horizontally placed on suitable supports inside a salt-spray chamber (35 ± 2 °C, RH = 95–98%, NaCl = 5%), simulating a warm, humid, and chloride-rich environment. Electrodes were plasticine-sealed to prevent corrosion; exposure lasted 21 days. The measurements included both electrical impedance and free chloride concentration analysis and were carried out at 0 (i.e., start of test, after 28 days of curing), 7, 14, and 21 days. The latter was measured on 0–30 mm depth following the standard UNI 9944; powder samples (approximately 15 g each) were collected after drilling the dedicated specimens with the same compositions and the same exposure conditions of specimens for electrical impedance measurements. The analysis of free chloride content, expressed as wt% of the cement, was carried out after having put the powder sample in 60 ml of distilled water, mixed for 24 h, filtered and diluted in 100 ml of distilled water.

3.5. Capillary water absorption

Capillary water absorption test was carried out by placing concrete specimens horizontally in a closed container with distilled water (3.5 cm depth). At each test time (i.e., 0 - start of test, after 35 days of curing -, 10, 20, 30, and 60 min, 4, 6, 24, 48, 72, 96, 168, and 192 h and then, twice per week for a total duration of 35 days), concrete specimens were weighed before being subjected to electrical impedance measurement. The water absorbed per unit area (Q_i [kg/m^2]) was derived in compliance to the standard EN 15801.

3.6. Water penetration (wet/dry cycles)

Concrete specimens were inserted inside a closed plastic box containing water (9 cm depth, maintained constant by adding the absorbed one). The specimens were horizontally placed on cylindrical supports to ensure the absorption of water from the bottom surface and were exposed to 4 weekly wet/dry cycles (2 days wet and 5 days dry). Electrical measurements were carried out 2 times per each cycle, i.e., immediately after the extraction from water and just before the next immersion, for a total of 4 cycles.

3.7. Chloride penetration (wet/dry cycles)

To simulate a chloride penetration in a cyclically wet and dry environment, concrete specimens were inserted inside a closed plastic box containing a 3.5% NaCl solution (9 cm depth, maintained constant by adding the absorbed one). The test procedure was the same adopted in water penetration test (wet/dry cycles), with the difference of 3.5% NaCl solution instead of water. As for salt-spray chamber test, electrodes for electrical impedance measurement were plasticine-sealed to prevent possible corrosion. Free chloride concentration analysis was performed in the same manner as for salt-spray chamber, on 0–30 mm depth, at the same test times of electrical measurements.

4. Results and discussion

4.1. Effect of different types of biochar on mechanical and electrical properties of mortars

Results in terms of compressive strength and electrical impedance of mortars are reported in Fig. 6a and Fig. 6b, respectively. It is possible to observe that the different types of fillers added at 0.5 vol% provide to mortars a different behaviour both in terms of compressive strength and electrical impedance. After 35 days of curing, GCH and RAV biochar do not alter the mechanical strength and decrease the electrical impedance

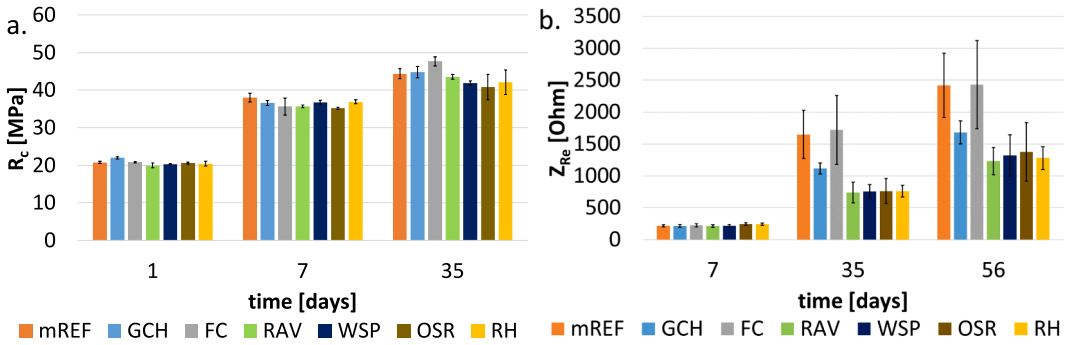

Fig. 6. a. compressive strength and b. electrical impedance of mortar specimens cast with different carbon-based fillers.

of mortars compared to mREF, whereas FC biochar slightly increases the compressive strength of mortar but does not affect the electrical impedance. Conversely, the other types of biochar (i.e., WSP, OSR, and RH) have negative effects on compressive strength, even if they contribute to decrease the mortars electrical impedance by approximately 50% at the end of the test. The increase of compressive strength and the decrease of electrical impedance of the mortar manufactured with GCH confirms that GCH is a good low-cost carbonaceous by-product for manufacturing low-resistive composites [23]. On the contrary, the different effects obtained by the other types of biochar could be related to the different raw materials used for their production and the different pyrolysis temperature used for their manufacturing. For example, Pariyar et al. [38] stated that paper sludge and poultry litter biochar have a high ash content, whereas saw dust, rice husk, and food waste biochar show a high fixed carbon value. Moreover, the higher the pyrolysis temperature, the higher the aromaticity degree and the lower the polarity, making biochar more suitable for carbon sequestration and agricultural applications.

Given the obtained results, RAV biochar was chosen to be further employed in concretes, because it provides to mortars the best compromise between electrical and mechanical performances. In fact, RAV lowers the electrical impedance by 49% without significantly decreasing the compressive strength of mortar. These results are even better than those provided by the previously adopted GCH, which decreases electrical impedance of approximately 30% and, as RAV, leaves compressive strength almost unaltered (Fig. 6).

4.2. *Curing period: mechanical strength and electrical impedance of concretes*

After the preliminary tests on mortars, RAV biochar was used in combination to RCF to manufacture concretes. Results obtained during the curing period are reported in Fig. 7 and Fig. 8. During the first 28 days of curing, both compressive strength (Fig. 7a) and electrical impedance of concrete specimens (Fig. 8) increase, as expected. After 28 days of curing, the mix with fibres (RCF EDC) reaches a compressive strength 17% lower than REF EDC (Fig. 7a). Perhaps, the great amount of PC2 and PC3 admixtures increased the mixtures porosity. As a matter of fact the total pore volume increases (Fig. 9a), the volume of macropores (pores with $d > 1$ μm [39]) is much higher in this mix with respect to the others (Fig. 9b) and the corresponding hardened density is slightly lower (Table 3). In order to avoid the formation of air bubbles, defoaming agents can be introduced into the concrete mix-design [40]; however, the addition of BCH in concrete seems to compensate for this issue both in BCH EDC and RCF + BCH EDC specimens. Probably BCH, being a filler, provides to concrete the so-called "filler effect" [41] and the formation of more hydration products thanks to the "nucleation effect" [42], which densifies the microstructure (Table 3) moving the main porosity to smaller diameters (Fig. 9b).

In any case, the use of RCF does not lower the tensile strength of concrete (Fig. 7b); in fact, the bridging effect of fibres increases the material strength under tension and reduces the cracks propagation within the matrix [2,20,43]. Moreover, the combined use of RCF and BCH gives a synergistic effect on tensile splitting behaviour, which increases of approximately 19% compared to REF EDC mix.

As electrical impedance (Fig. 8a) is concerned, after 28 days of curing the addition of RCF contributes to decrease the Z_{Re} value of 15%. The good electrical properties supplied by the addition of RCF to cement-based matrixes have already been reported in the literature, also at the low dosage of 0.05% volume content [20]. On the contrary, BCH causes an increase of electrical impedance of approximately 19%, which is in contrast with the results previously obtained in mortars specimens (Section 4.1). Some hypotheses to explain these results are proposed hereafter. The combined use of carbon-based additions does not improve the performance obtained with RCF alone, since Z_{Re} value decreases by only 8% after 28 days of curing. During the first 28 days, moisture acts as the main factor influencing the electrical impedance results, particularly when RCF were added alone. Indeed, the effect of the combined use of conductive additions in decreasing electrical impedance of concrete becomes more evident after 28 days of curing (Fig. 8b). The enhanced

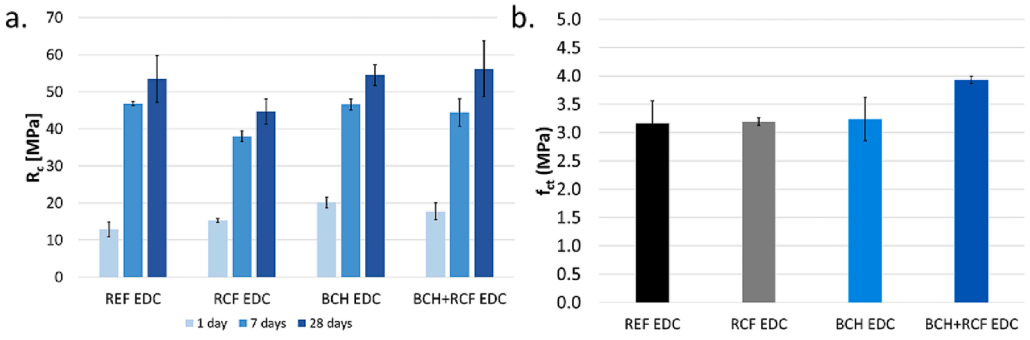

Fig. 7. a. compressive strength measured during curing period and b. tensile strength measured at 28 days of curing.

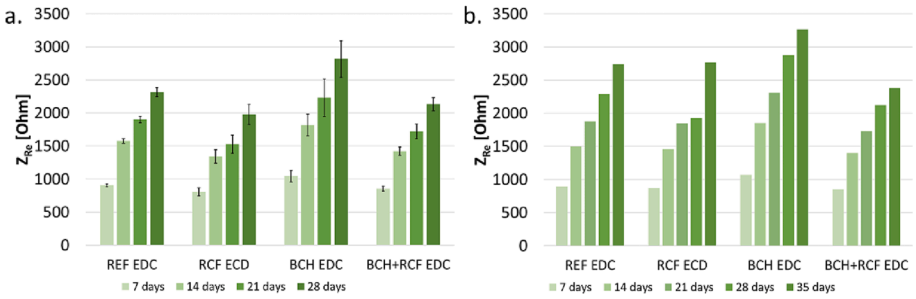

Fig. 8. Electrical impedance measured a. during 28 days of curing and b. up to 35 days after casting in dedicate concrete specimens.

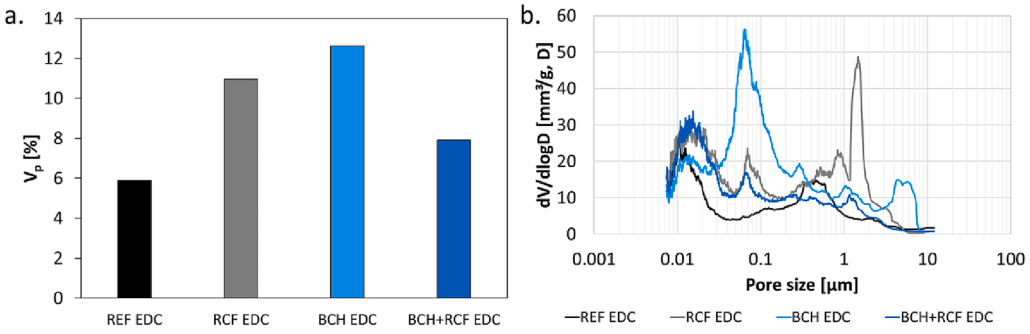

Fig. 9. a. total porosity and b. pore size distribution after 28 days of curing.

Table 3
Hardened density after 28 days of curing.

Mixture	Density [kg/m^3]
REF EDC	2372
RCF EDC	2309
BCH EDC	2363
RCF + BCH EDC	2373

effect of conductive additions on electrical properties of concretes when used in combination has already been found by authors in [23], where RCF were added to concretes together with GCH. This confirms what was reported by Wen and Chung: the combined use of conductive fibres and fillers can enhance the electrical properties of the final material [44]. Indeed, considering the results obtained on concrete specimens dedicated to the curing monitoring (Fig. 8b), from 28 to 35 days it is possible to observe a great increase of electrical impedance value of RCF EDC, which becomes similar to that of REF EDC. Furthermore, BCH EDC continues to show an increased Z_{Re} value compared to the plain concrete. As reported by Belli et al. [45], when specimens are moist, water plays the predominant role on the measured electrical impedance values. Therefore, the contribution of conductive additions on the electrical properties of concretes is more visible in dried specimens. Moreover, the use of RCF and BCH together confirms to be the most effective solution since the electrical impedance decreases of about 13% with respect to REF EDC thanks to a combined effect.

Summarising, it is possible to state that the combined use of RCF and BCH provides an enhanced effect on both electrical and mechanical properties of concrete, compared to concretes manufactured with only one carbon-based addition. Moreover, it is worthy to underline that BCH does not show the same performance in concrete and mortar; this could be attributed to multiple reasons:

- Different cement type: CEM II A-LL 42.5R (used for mortars cast) seems to be more conductive than CEM II/C-M (S-LL) (used for concretes cast). As reported by Azarsa and Gupta [46], the addition of supplementary cementitious materials such as blast furnace slag (which is present in CEM II/C-M (S-LL)) and fly ash decreases the permeability, thus reduces pores solution, leading to a higher electrical resistivity as a consequence of the reduced capillary porosity and hydroxyl ions (OH^-);
- Different w/c ratios: 0.50 in mortars and 0.42 in concretes, which determine a higher porosity in mortars influencing the effect of BCH in the two materials;
- Different curing conditions: mortars are kept at RH = 95 ± 5% for 7 days, whereas concretes for 28 days. Consequently, in mortars the effect of BCH is visible already after 7 days, whereas in concretes it appears only after the wet curing and when BCH is coupled with RCF;
- Concretes are cast with bigger aggregates and a higher aggregate to cement ratio; these factors probably make the BCH distribution less homogeneous in the concrete volume, and thus less efficient. This is confirmed also by Chiarello et al. and Baeza et al., who stated that aggregates cause an increase of concrete electrical resistivity. Therefore, a higher conductive additions quantity is needed to reach the expected self-sensing ability with respect to mortars [47,48].

4.3. Exposure tests

After 28 days of curing, specimens were exposed to different accelerated durability tests. Results obtained are reported hereafter.

4.3.1. Accelerated carbonation

The carbonation of specimens increases in time (Fig. 10a), as expected. The REF EDC concrete specimen is the one less subjected to carbonation, whereas all the other specimens manufactured with conductive additions increase the susceptibility to the CO_2-rich environment. In general, carbonation increases when RCF and BCH are added both alone and together. For the RCF EDC specimen, this is related to its higher porosity (Fig. 9a), which facilitates the ingress of CO_2. On the contrary, the higher carbonation of BCH EDC and RCF + BCH EDC is related both to their high total porosity (Fig. 9a) and to the physical properties of biochar. The pyrolysis process provides BCH particles with a high specific surface area and a porous structure,

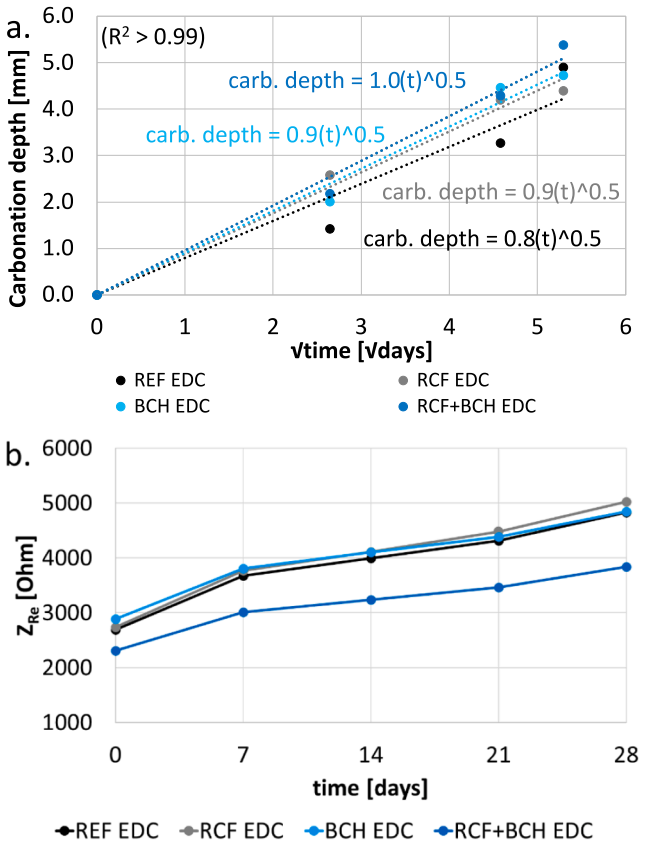

Fig. 10. Results of accelerated carbonation test: a. carbonation depth and b. electrical impedance over test time.

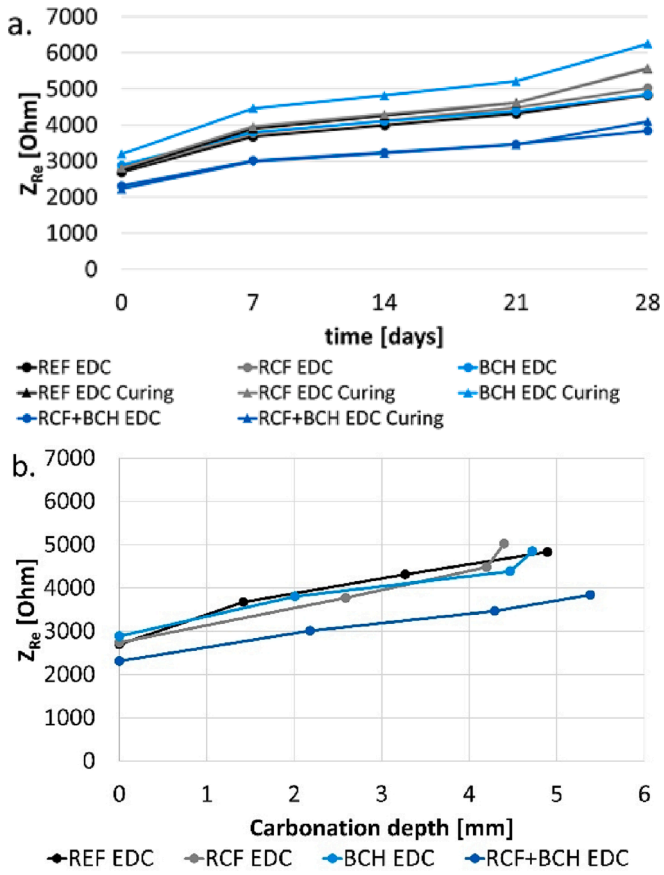

Fig. 11. a. comparison between electrical impedance measured during accelerated carbonation test and during curing and b. correlation between electrical impedance and carbonation depth.

conferring very good adsorption properties [42]. In fact, in construction materials biochar is used also as CO_2 catcher [49,50].

While carbonation occurs, the electrical impedance of concretes should increase (Fig. 10b) since carbonation decreases the ion concentration of the pore solution [51] owing to the transformation of $Ca(OH)_2$ in $CaCO_3$ that precipitates inside. In general, the trend showed by specimens is the same for each composition: during the first week of exposure, the curve is slightly more leaning, whereas for long periods of time it changes its slope. This happens because during the first 7 days the materials are subjected to a change in the environmental conditions they are exposed to, moving from RH > 95% of wet curing to an unsaturated environment (RH = 60 ± 10% in the carbonation chamber). The internal moisture is thus free to evaporate, faster at the beginning of the test.

Comparing electrical impedance values measured during accelerated carbonation test and curing (Fig. 11a), similar trends in terms of curve slopes can be observed. This means that the specimens similarly lose water due to evaporation and cement hydration. Again, the electrical impedance variation seems to be more sensitive to water content and the hydration degree of cement paste than to carbonation depth. The correlation between electrical impedance and carbonation depth is reported in Fig. 11b. The progress of carbonation can be detected as an increase of electrical impedance. Moreover, as already found in a previous experimentation [23], for longer exposure times the trends of the Z_{Re} values change their slope, since both carbonation and curing sum up their effects on electrical impedance values resulting in an increase of Z_{Re}.

4.3.2. Salt-spray chamber

The free chloride content on cement weight measured during the exposure in the salt-spray chamber is reported in Fig. 12a. As expected, the free chloride concentration increases with exposure time. The highest chloride amount is recorded in RCF EDC specimen, followed by REF EDC, BCH EDC, and RCF + BCH EDC specimens. The specimen manufactured with RCF has a higher porosity than REF EDC (Fig. 9a), which enables chloride ions to penetrate easier within the matrix. When RCF and BCH are both added to concrete, chloride penetration is reduced owing to the finer concrete microstructure (Fig. 9b).

Electrical impedance progressively decreases with chloride penetration (Fig. 12b), as reported in literature [52], because chloride ions contribute to increase the ionic conductivity of concrete. The most evident decrease of electrical impedance takes place between 0 and 7 days, since the specimens move from dry to wet conditions and it is equal to 74%, 78%, 72%, and 80% for REF EDC, RCF EDC, BCH EDC, and RCF + BCH EDC, respectively. After 7 days, although chloride content increases over time, electrical impedance remains almost constant. This means that electrical impedance values are more affected by water than by chlorides content. From 14 to 21 days, electrical impedance moves towards higher values; at the same time free chloride concentration stabilizes. Therefore, the chloride solution does not affect the impedance measurement anymore, but only the internal microstructural changes of concrete (reduction of porosity, determined by the progressive hydration related to curing).

Comparing the results of Z_{Re} measured both during curing and exposure in the salt-spray chamber (Fig. 13a), electrical impedance values follow the same increasing trend between 14 and 21 days. This is associated with the continuous curing of specimens, giving a more and more dense microstructure, which determines the increase of Z_{Re} values in the two conditions. The correlation between electrical impedance and chloride content (Fig. 13b) shows that, when chloride-rich solution penetrates, electrical impedance decreases, but the changes in values are related to the changes of environmental conditions (dry and wet).

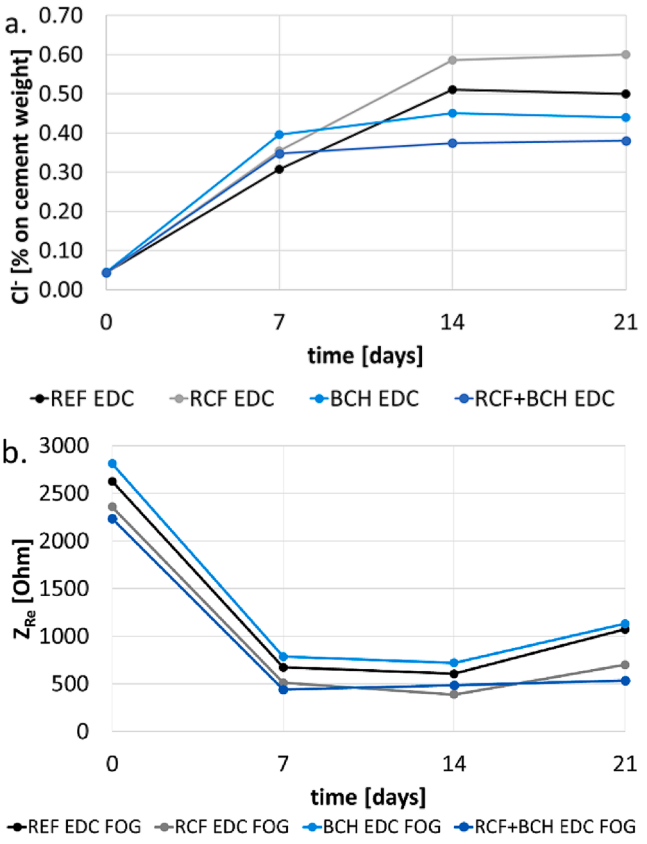

Fig. 12. Results of salt-spray chamber test: a. free chloride content on cement weight and b. electrical impedance over test time.

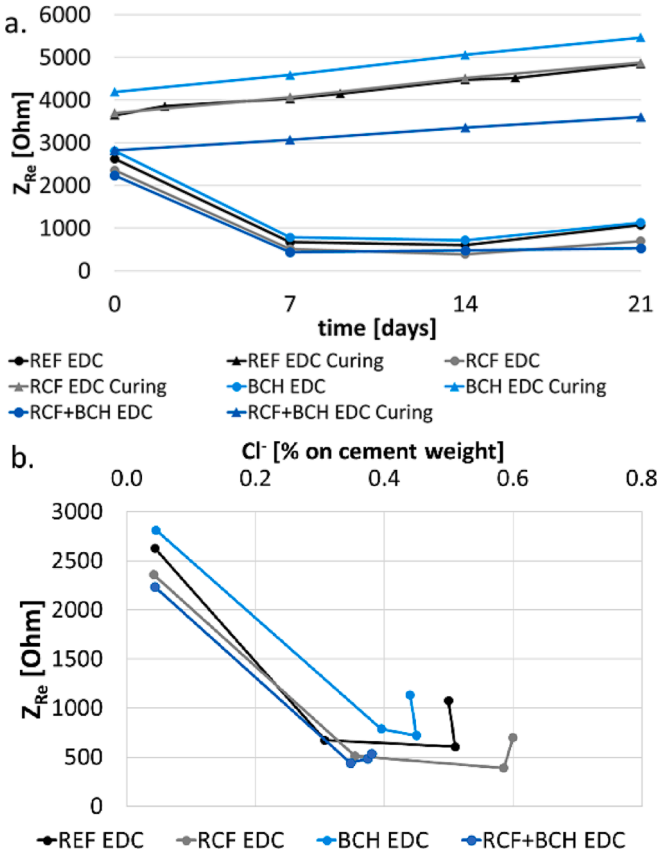

Fig. 13. a. comparison between electrical impedance measured during salt-spray chamber test and during curing and b. correlation between electrical impedance and chloride content on cement weight.

Moreover, the initial penetration can be detected similarly in all the compositions. Even if chlorides continue penetrating during the exposure, after one week of exposure the electrical impedance values stabilize, because they are more affected by the water content than by the chlorides content. After an additional week (last point of each curve), the curing effect on the measured electrical impedance prevails and the electrical impedance values begin to increase, since chlorides content stabilizes. Especially when RCF and BCH are added together, chloride penetration is reduced; this is due to the "barrier effect" of carbon-based additions, which absorb the solution and slow down its penetration into concrete deeper layers by retaining it [53].

4.3.3. *Capillary water absorption*

As reported in literature [54], electrical impedance progressively decreases when water is absorbed, since an increased moisture content improves the ion mobility [46]. Both RCF and BCH increase water absorption of concretes, especially when used alone. This negative impact was already found by the present authors [23] and could be attributable to different causes: the relative high quantity of biochar [53] and also the higher total porosity (Fig. 9a), besides bigger pores, which increase the water absorption of the composite material. Moreover, carbon-based materials are reported to have a good water absorption capacity making them more prone to the water capillary suction [20,42,55]. On the other hand, the combined use of BCH and RCF reduces the concrete water absorption, achieving values similar to REF EDC. This can be attributed to the microstructural refinement of the paste (Fig. 9), which shortens/segments the porosity continuous paths, hindering the ingress of water through capillary action. Concrete specimens continue to absorb water for the whole test duration (35 days, i.e., 840 h), without reaching saturation; indeed, the Q_i values continue to increase without stabilizing (Fig. 14a). Most of the absorption occurs within the first 72 h; during this period electrical impedance is sensitive to water penetration, in fact Z_{Re} decreases, (Fig. 14b). After 72 h, electrical impedance inverts its trend, probably due to a decrease of the outdoor temperature ($\Delta T \sim 5$ °C) but also to the curing process (Fig. 15a): Z_{Re} increases in time because of the continue hydration of cement and the evaporation of internal water [56]. After 3 days, electrical impedance seems more sensitive to curing than to further capillary water absorption probably because specimens are wet and kept at RH > 95% in closed containers. In any case, during the first days (when capillary water absorption begins) the significative decrease of Z_{Re} values suggests the ingress of water inside the specimens.

The correlation between electrical impedance and water absorbed per unit area (up to 72 h of test, thus when water penetration is the predominant effect) is reported in Fig. 15b. It is possible to observe that electrical impedance slightly decreases while water penetrates, because concrete specimens move from dry to wet conditions. At low amounts of absorbed water ($0 < Q_i < 0.15$ kg/m^2) (short contact time), conductive material additions seem to help the sensing to water absorption. In fact, the slope of the curve is more leaning compared to that of REF EDC, probably because of the faster water absorption. Instead, at higher amounts of absorbed water ($Q_i > 0.15$ kg/m^2) (long contact time), the slope of REF EDC curve becomes the most leaning. Indeed, electrical impedance further decreases, probably because the sensing volume contains more water than the other specimens containing conductive additions. This fact, already found by the present authors [23], could be explained again with the water retention capability of the conductive additions [10], which reduces the penetration depth of water giving a sort of "barrier effect" [23,53].

4.3.4. *Water penetration (wet/dry cycles)*

In this testing campaign, REF EDC and RCF EDC specimens show similar water absorption coefficients, whereas absorption is increased in

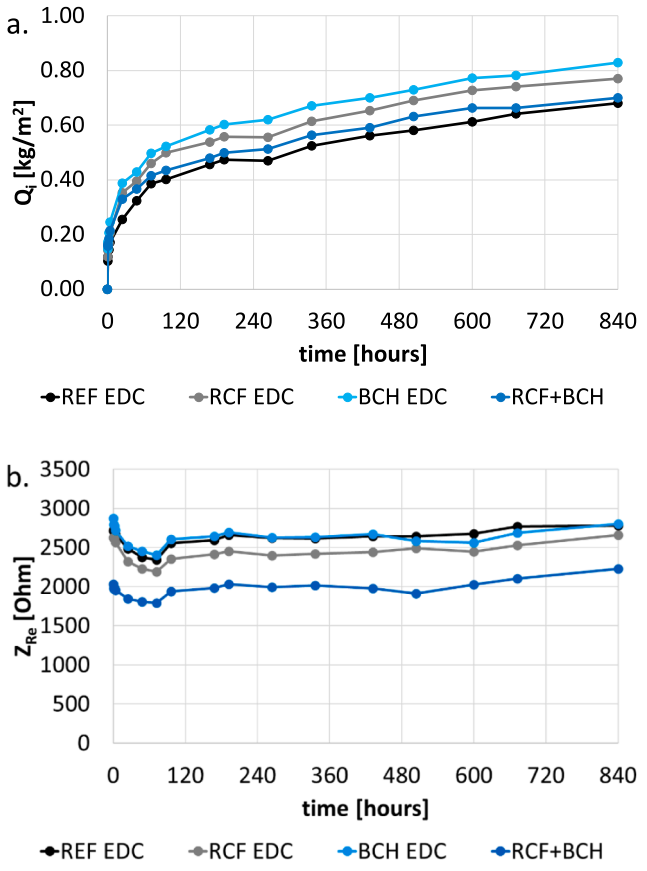

Fig. 14. Results of capillary water absorption tests: a. water absorbed per unit area and b. electrical impedance during test time.

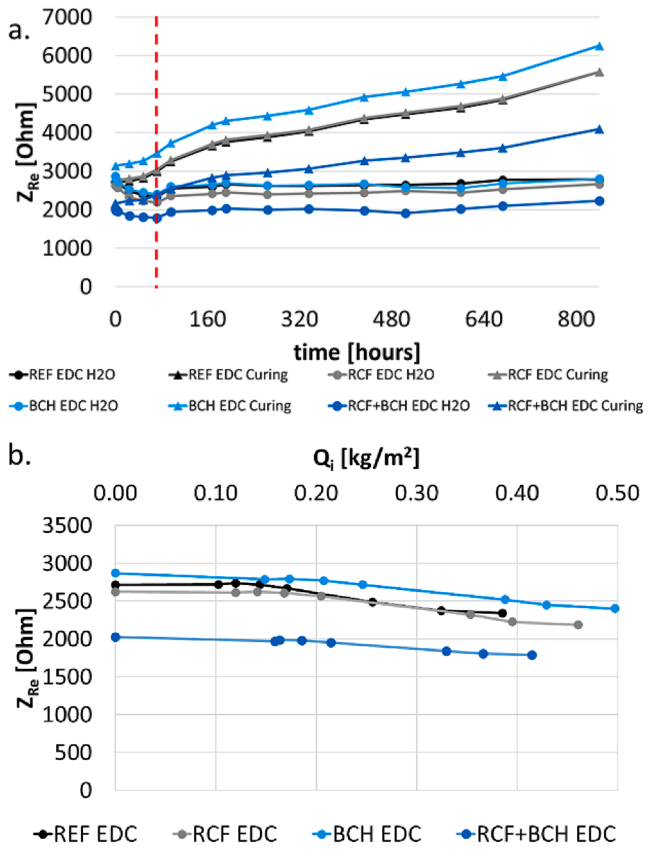

Fig. 15. a. comparison between electrical impedance measured during capillary water absorption test and curing time (red line is positioned at t = 72 h) and b. correlation between electrical impedance and water absorbed per unit area (up to 72 h of test). (For interpretation of the references to colour in this figure legend, the reader is referred to the web version of this article.)

both the specimens containing BCH (i.e., BCH EDC and RCF + BCH EDC, Fig. 16a, where Q_i values are reported only for wet concretes). This is due to the high water absorption capacity of biochar [10]. Electrical impedance measurements can detect and follow very well the wet/dry conditions of concrete, (Fig. 16b). As expected [54], just after the first immersion (2 days after time 0) the electrical impedance decreases. Again, this result is related to the water absorption mechanism. Moreover, for all compositions when specimens are wet (i.e., after 2, 9, 16, and 23 days) the value of Z_{Re} is lower than when specimens are dry (i.e., after 7, 14, 21, and 28 days), as it is visible in Fig. 16b. However, after 7 days of exposure (i.e., the first wet/dry cycle) the electrical impedance trend increases for all the compositions (Fig. 16b, dashed curves) both in wet and in dry conditions. Also in this case, the result is related to the effect of curing/hydration of concrete, which increases the compactness of the matrix by reducing the porosity of the material in time.

The correlation between electrical impedance of specimens in wet condition and water absorption is reported in Fig. 17. It is clearly visible that at the beginning of the test, namely 2 days after immersion, while water penetrates electrical impedance decreases, in fact specimens move from dry to wet conditions. After the first wet/dry cycle, the electrical impedance trend increases, even if the water absorption slightly increases (Fig. 16a). This result suggests that the curing effect prevails on water absorption effect.

4.3.5. *Chloride penetration (wet/dry cycles)*

After wet/dry cycle in the 3.5% NaCl solution, all concrete specimens contain a similar free chloride amount (Fig. 18a), which ranges from 0.26% to 0.29% by cement weight. These concentrations are lower than those measured after the salt-spray chamber test (Fig. 12a), which range from 0.38% to 0.60% by cement weight. This is related to the short period of time that specimens are in contact with the solution. As noticed in water penetration during wet/dry cycles test (Fig. 16b), electrical impedance values follow very well the wet/dry conditions of concrete specimens (Fig. 18b), with lowest values during wet periods. In presence of chlorides, the amplitude of the oscillations in the electrical impedance values are higher than in simple water. In fact, when specimens are exposed to water the difference of Z_{Re} values between wet and dry periods attains around 23%, whereas when they are exposed to the chloride-rich solution the difference of Z_{Re} values between wet and dry periods reaches 40–45%. This result is related to the fact that chlorides contribute to decrease electrical impedance and this effect sums up to the water ingress. However, for all the compositions, an increasing electrical impedance trend for both wet and dry periods can be observed as for wet/dry cycles in water. This means that curing affects electrical impedance values more than chloride solution penetration, since the electrical impedance increases even if chlorides content increases.

The correlation between electrical impedance of specimens in dry condition and free chloride concentration is reported in Fig. 19. It can be noticed that dry conditions highlight the effect of chloride penetration, which otherwise could be masked by water. While chloride-rich solution penetrates, electrical impedance decreases and follows the wet/dry cycles trend, as observable in Fig. 18b. However, in this testing campaign the chloride penetration is very limited and after few cycles electrical impedance trend is increasing. This happens probably for two reasons: curing becomes the prevailing effect and the chloride-rich solution does not reach the sensing volume interested by the Wenner's method-based configuration.

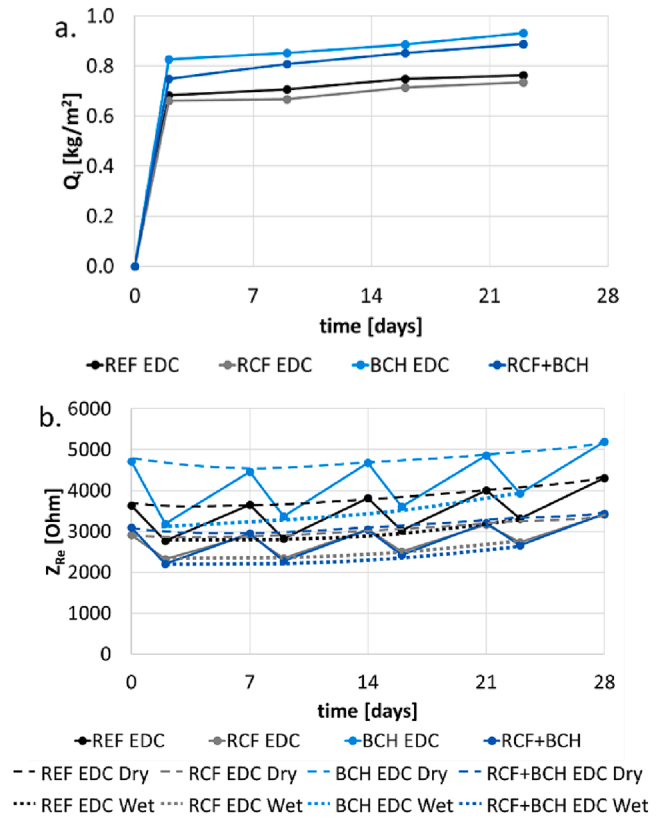

Fig. 16. Results of water penetration (wet/dry cycles) test: a. water absorbed per unit area and b. electrical impedance over time.

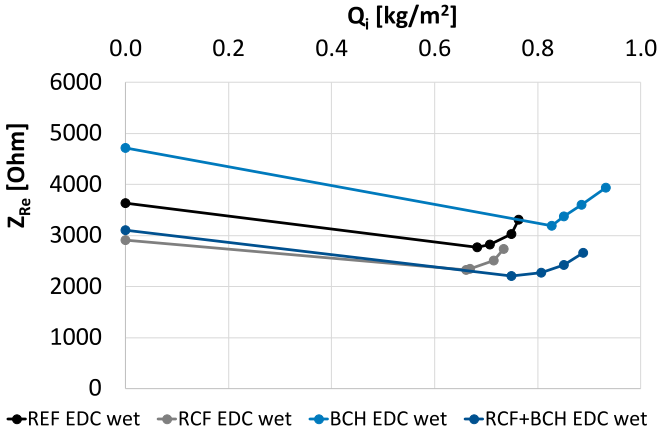

Fig. 17. Correlations between electrical impedance and water absorbed per unit area during wet periods of test.

5. Conclusions

Recycled carbon fibres (RCF) and biochar (BCH) have been used both alone and coupled together to manufacture low-resistive cement-based mixes and the relative performances have been evaluated in terms of compressive and tensile strengths, durability, and material electrical impedance during curing (28 days) and accelerated degradation tests.

From the obtained results it is possible to state that:

- The chosen biochar provides to mortars a decreased electrical impedance (approximately 45% with respect to reference mix design) without affecting the compressive strength;

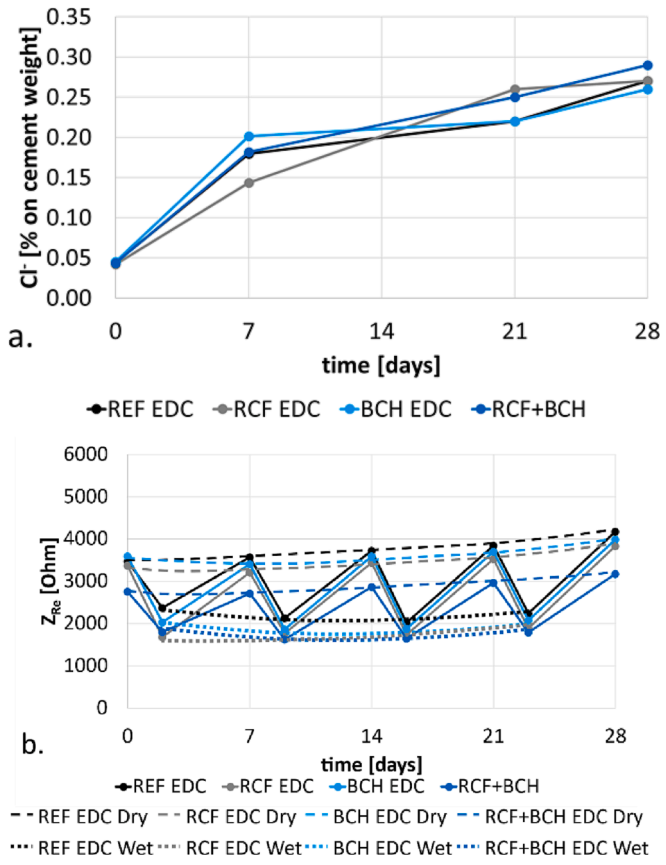

Fig. 18. Results of chloride penetration (wet/dry cycles) test: a. free chloride content on cement weight and b. electrical impedance over time.

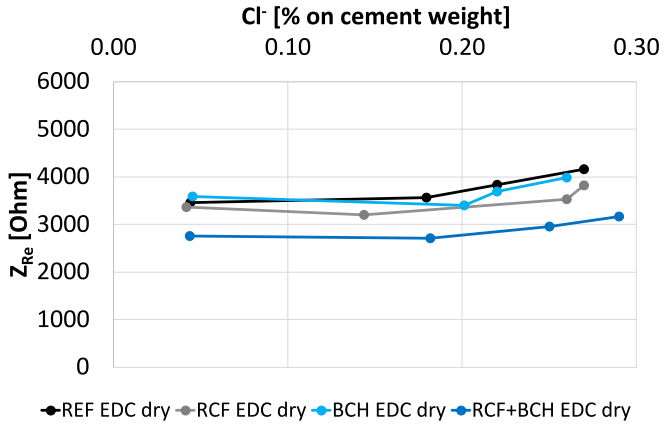

Fig. 19. Correlations between electrical impedance and free chloride content on cement weight during dry periods.

- Moisture content has a predominant effect in the measured electrical impedance of concretes; the effect of carbon-based additions becomes more visible after the first 28 days of curing (the electrical impedance decrease is of approximately 13% at 35 days when RCF and BCH are used in combination);
- Compressive strength values are comparable among the different concrete compositions, with the only exception of RCF (decrease of approximately 17%, due to the higher total porosity and the bigger pore size);
- The combined use of RCF and BCH enhances (approximately 24%) the tensile strength of concretes.

Concerning durability, it can be summarised that:

- Conductive additions seem to increase water absorption, probably because RCF increases the porosity of the specimens, whereas BCH has a porous structure favouring water retention; on the other hand, they seem to decrease the water penetration depth, with a sort of "barrier effect";
- Biochar decreases chloride penetration in salt-spray chamber test thanks to its filler effect;
- Conductive additions seem to slightly accelerate carbonation because RCF increases the porosity of the specimens and BCH is a CO_2 catcher.

The findings suggest that both RCF and BCH are suitable materials to enhance concrete electrical properties, especially when used in combination. The increase of material electrical conductivity is very important for self-sensing applications, allowing to perform the measurements with low-cost instrumentation, given the better Signal-to-Noise Ratio (SNR). This is particularly important to develop a long-term monitoring system based on electrical impedance measurement in a distributed sensors network configuration, in order to regularly collect data directly linked to the concrete health status. This allows to foresee any possible issue related to durability and integrity of the structure itself, hence acting in a timely and effective way, optimizing the lifecycle of the structure itself. Moreover, the configuration adopted for electrical impedance measurements (i.e., Wenner's method, 10 kHz measurement frequency) confirms to be suitable for concrete monitoring purposes. The contaminants penetration does not spoil electrical impedance measurement, since the results agree with what expected: electrical impedance decreases with water and chloride penetration by aerosols, whereas it increases with carbonation and follows very well the wet/dry cycles in water and chloride-rich solutions. However, it is worthy to stress that the ingress of contaminants is reflected in electrical impedance changes only if the substances reach the sensing volume, otherwise the results will be affected only by curing and environmental conditions (temperature and humidity). Furthermore, if different factors act simultaneously, the contribution of each factor in the modification of electrical impedance cannot be distinguishable in the measurement. Therefore, the occurrence of a potential hazardous event in a real application can be inferred from a change in the electrical impedance trend but the specific cause of such modification should be investigated through deeper analyses (e.g., inspection procedures).

CRediT authorship contribution statement

A. Mobili: Conceptualization, Methodology, Software, Validation, Formal analysis, Investigation, Data curation, Writing – original draft. **G. Cosoli:** Conceptualization, Methodology, Software, Validation, Formal analysis, Investigation, Data curation, Writing – original draft. **N. Giulietti:** Conceptualization, Methodology, Software, Validation, Formal analysis, Investigation, Data curation, Writing – review & editing. **P. Chiariotti:** Conceptualization, Methodology, Software, Validation, Formal analysis, Data curation, Writing – review & editing, Supervision. **T. Bellezze:** Conceptualization, Data curation, Resources, Writing – review & editing, Supervision. **G. Pandarese:** Investigation, Writing – review & editing. **G.M. Revel:** Conceptualization, Resources, Writing – review & editing, Supervision, Funding acquisition. **F. Tittarelli:** Conceptualization, Resources, Writing – review & editing, Supervision.

Declaration of Competing Interest

The authors declare that they have no known competing financial interests or personal relationships that could have appeared to influence the work reported in this paper.

Data availability

Data will be made available on request.

Acknowledgements

This research activity was carried out within the EnDurCrete (New Environmental friendly and Durable conCrete, integrating industrial by-products and hybrid systems, for civil, industrial and offshore applications) project, funded by the European Union's Horizon 2020 research and innovation programme under grant agreement n° 760639.

Authors would like to thank HeidelbergCement AG, NuovaTesi System and Sika groups for having provided cement, aggregates and admixtures, respectively, to cast concrete. Moreover, the authors wish to thank Procotex Belgium SA for the recycled carbon fibers, RES Italia for RAV biochar, Carbonitalia srl for FC biochar, and UK Biochar Research Center for WSP, OSR, and RH types of biochar kindly offered for this work.

References

[1] D.D.L. Chung, Carbon materials for structural self-sensing, electromagnetic shielding and thermal interfacing, Carbon N. Y. 50 (2012) 3342–3353, https://doi.org/10.1016/j.carbon.2012.01.031.
[2] A. Mobili, G. Cosoli, T. Bellezze, G.M. Revel, F. Tittarelli, Use of gasification char and recycled carbon fibres for sustainable and durable low-resistivity cement-based composites, J. Build. Eng. 50 (2022), 104237, https://doi.org/10.1016/j.jobe.2022.104237.
[3] O. Mašek, V. Budarin, M. Gronnow, K. Crombie, P. Brownsort, E. Fitzpatrick, P. Hurst, Microwave and slow pyrolysis biochar - Comparison of physical and functional properties, J. Anal. Appl. Pyrolysis. 100 (2013) 41–48, https://doi.org/10.1016/j.jaap.2012.11.015.
[4] M. Tripathi, J.N. Sahu, P. Ganesan, Effect of process parameters on production of biochar from biomass waste through pyrolysis: A review, Renew. Sustain. Energy Rev. 55 (2016) 467–481, https://doi.org/10.1016/j.rser.2015.10.122.
[5] H. Maljaee, R. Madadi, H. Paiva, L. Tarelho, V.M. Ferreira, Incorporation of biochar in cementitious materials: A roadmap of biochar selection, Constr. Build. Mater. 283 (2021), 122757, https://doi.org/10.1016/J.CONBUILDMAT.2021.122757.
[6] R.A. Mensah, V. Shanmugam, S. Narayanan, S.M.J. Razavi, A. Ulfberg, T. Blanksvärd, F. Sayahi, P. Simonsson, B. Reinke, M. Försth, G. Sas, D. Sas, O. Das, Biochar-Added Cementitious Materials—A Review on Mechanical, Thermal, and Environmental Properties, Sustain. 2021, Vol. 13, Page 9336. 13 (2021) 9336. https://doi.org/10.3390/SU13169336.
[7] D. Winters, K. Boakye, S. Simske, Toward Carbon-Neutral Concrete through Biochar–Cement–Calcium Carbonate Composites: A Critical Review, Sustain. 2022, Vol. 14, Page 4633. 14 (2022) 4633. https://doi.org/10.3390/SU14084633.
[8] S. Gupta, H.W. Kua, S.D. Pang, Effect of biochar on mechanical and permeability properties of concrete exposed to elevated temperature, Constr. Build. Mater. 234 (2020), 117338, https://doi.org/10.1016/j.conbuildmat.2019.117338.
[9] A. Akhtar, A.K. Sarmah, Novel biochar-concrete composites: Manufacturing, characterization and evaluation of the mechanical properties, Sci. Total Environ. 616–617 (2018) 408–416, https://doi.org/10.1016/j.scitotenv.2017.10.319.
[10] S. Gupta, H.W. Kua, Effect of water entrainment by pre-soaked biochar particles on strength and permeability of cement mortar, Constr. Build. Mater. 159 (2018) 107–125, https://doi.org/10.1016/j.conbuildmat.2017.10.095.
[11] W.C. Choi, H. Do Yun, J.Y. Lee, Mechanical Properties of Mortar Containing Bio-Char From Pyrolysis, J. Korea Inst. Struct. Maint. Insp. 16 (2012) 67–74.
[12] M. Zhao, Y. Jia, L. Yuan, J. Qiu, C. Xie, Experimental study on the vegetation characteristics of biochar-modified vegetation concrete, Constr. Build. Mater. 206 (2019) 321–328, https://doi.org/10.1016/j.conbuildmat.2019.01.238.
[13] D. Cuthbertson, U. Berardi, C. Briens, F. Berruti, Biochar from residual biomass as a concrete filler for improved thermal and acoustic properties, Biomass Bioenergy. 120 (2019) 77–83, https://doi.org/10.1016/j.biombioe.2018.11.007.
[14] S. Gupta, H.W. Kua, Factors Determining the Potential of Biochar As a Carbon Capturing and Sequestering Construction Material: Critical Review, J. Mater. Civ. Eng. 29 (2017) 04017086, https://doi.org/10.1061/(asce)mt.1943-5533.0001924.
[15] H.W. Kua, S. Gupta, A.N. Aday, W.V. Srubar, Biochar-immobilized bacteria and superabsorbent polymers enable self-healing of fiber-reinforced concrete after multiple damage cycles, Cem. Concr. Compos. 100 (2019) 35–52, https://doi.org/10.1016/j.cemconcomp.2019.03.017.
[16] D. Falliano, D. De Domenico, A. Sciarrone, G. Ricciardi, L. Restuccia, G. Ferro, J.-M. Tulliani, E. Gugliandolo, Influence of biochar additions on the fracture behavior of foamed concrete, Frat. Ed Integrità Strutt. 51 (2020) 189–198, https://doi.org/10.3221/IGF-ESIS.51.15.
[17] S. Muthukrishnan, S. Gupta, H.W. Kua, Application of rice husk biochar and thermally treated low silica rice husk ash to improve physical properties of cement mortar, Theor. Appl. Fract. Mech. 104 (2019), 102376, https://doi.org/10.1016/J.TAFMEC.2019.102376.

[18] L. Mo, J. Fang, B. Huang, A. Wang, M. Deng, Combined effects of biochar and MgO expansive additive on the autogenous shrinkage, internal relative humidity and compressive strength of cement pastes, Constr. Build. Mater. 229 (2019), 116877, https://doi.org/10.1016/J.CONBUILDMAT.2019.116877.
[19] B. Han, X. Yu, J. Ou, Carbon-Fiber-Based Self-Sensing Concrete, in: Self-Sensing Concr. Smart Struct., Elsevier, 2014: pp. 231–269. Doi: 10.1016/b978-0-12-800517-0.00008-3.
[20] A. Belli, A. Mobili, T. Bellezze, F. Tittarelli, Commercial and recycled carbon/steel fibers for fiber-reinforced cement mortars with high electrical conductivity, Cem. Concr. Compos. 109 (2020), 103569, https://doi.org/10.1016/j.cemconcomp.2020.103569.
[21] R. Merli, M. Preziosi, A. Acampora, M.C. Lucchetti, E. Petrucci, Recycled fibers in reinforced concrete: A systematic literature review, J. Clean. Prod. 248 (2020), 119207, https://doi.org/10.1016/j.jclepro.2019.119207.
[22] Global Recycled Carbon Fiber Market, 2021-2026, (n.d.). https://www.marketsandmarkets.com/Market-Reports/recycled-carbon-fiber-market-212462057.html (accessed February 24, 2023).
[23] A. Mobili, G. Cosoli, N. Giulietti, P. Chiariotti, G. Pandarese, T. Bellezze, G. M. Revel, F. Tittarelli, Effect of Gasification Char and Recycled Carbon Fibres on the Electrical Impedance of Concrete Exposed to Accelerated Degradation, Sustainability. 14 (2022), https://doi.org/10.3390/su14031775.
[24] M. Nematian, C. Keske, J.N. Ng'ombe, A techno-economic analysis of biochar production and the bioeconomy for orchard biomass, Waste Manag. 135 (2021) 467–477, https://doi.org/10.1016/j.wasman.2021.09.014.
[25] G. Habert, C. Billard, P. Rossi, C. Chen, N. Roussel, Cement production technology improvement compared to factor 4 objectives, Cem. Concr. Res. 40 (2010) 820–826, https://doi.org/10.1016/j.cemconres.2009.09.031.
[26] S.W. Tang, Y. Yao, C. Andrade, Z.J. Li, Recent durability studies on concrete structure, Cem. Concr. Res. 78 (2015) 143–154, https://doi.org/10.1016/j.cemconres.2015.05.021.
[27] D. Cusson, Z. Lounis, L. Daigle, Durability monitoring for improved service life predictions of concrete bridge decks in corrosive environments, Comput. Civ. Infrastruct. Eng. 26 (2011) 524–541, https://doi.org/10.1111/j.1467-8667.2010.00710.x.
[28] K. Osterminski, R.B. Polder, P. Schießl, Long term behaviour of the resistivity of concrete, Heron. 57 (2012) 211–230.
[29] M. Saleem, M. Shameem, S.E. Hussain, M. Maslehuddin, Effect of moisture, chloride and sulphate contamination on the electrical resistivity of Portland cement concrete, Constr. Build. Mater. 10 (1996) 209–214, https://doi.org/10.1016/0950-0618(95)00078-X.
[30] S. Rukzon, P. Chindaprasirt, R. Mahachai, Effect of grinding on chemical and physical properties of rice husk ash, Int. J. Miner. Metall. Mater. 16 (2009) 242–247, https://doi.org/10.1016/S1674-4799(09)60041-8.
[31] W. Xu, Y.T. Lo, D. Ouyang, S.A. Memon, F. Xing, W. Wang, X. Yuan, Effect of rice husk ash fineness on porosity and hydration reaction of blended cement paste, Constr. Build. Mater. 89 (2015) 90–101, https://doi.org/10.1016/j.conbuildmat.2015.04.030.
[32] G. Cosoli, A. Mobili, N. Giulietti, P. Chiariotti, G. Pandarese, F. Tittarelli, T. Bellezze, N. Mikanovic, G.M. Revel, Performance of concretes manufactured with newly developed low-clinker cements exposed to water and chlorides: Characterization by means of electrical impedance measurements, Constr. Build. Mater. 271 (2021), 121546, https://doi.org/10.1016/j.conbuildmat.2020.121546.
[33] G. Bolte, M. Zajac, J. Skocek, M. Ben Haha, Development of composite cements characterized by low environmental footprint, J. Clean. Prod. 226 (2019) 503–514, https://doi.org/10.1016/j.jclepro.2019.04.050.
[34] F. Wenner, A method for measuring Earth resistivity, J. Washingt. Acad. Sci. 5 (1915) 561–563.
[35] C.G. Berrocal, K. Hornbostel, M.R. Geiker, I. Löfgren, K. Lundgren, D.G. Bekas, Electrical resistivity measurements in steel fibre reinforced cementitious materials, Cem. Concr. Compos. 89 (2018) 216–229, https://doi.org/10.1016/j.cemconcomp.2018.03.015.
[36] UNI EN 13295 Determination of resistance to carbonation, (n.d.).
[37] N. Giulietti, P. Chiariotti, G. Cosoli, A. Mobili, G. Pandarese, F. Tittarelli, G. M. Revel, Automated measurement system for detecting carbonation depth: Image-processing based technique applied to concrete sprayed with phenolphthalein, Measurement. 175 (2021), 109142, https://doi.org/10.1016/j.measurement.2021.109142.
[38] P. Pariyar, K. Kumari, M.K. Jain, P.S. Jadhao, Evaluation of change in biochar properties derived from different feedstock and pyrolysis temperature for environmental and agricultural application, Sci. Total Environ. 713 (2020), 136433, https://doi.org/10.1016/j.scitotenv.2019.136433.
[39] R. Kumar, B. Bhattacharjee, Porosity, pore size distribution and in situ strength of concrete, Cem. Concr. Res. 33 (2003) 155–164, https://doi.org/10.1016/S0008-8846(02)00942-0.
[40] B. Łaźniewska-Piekarczyk, J. Szwabowski, The influence of the type of anti-foaming admixture and superplasticizer on the properties of self-compacting mortar and concrete, J. Civ. Eng. Manag. 18 (2012) 408–415, https://doi.org/10.3846/13923730.2012.698908.
[41] T. Tong, Z. Fan, Q. Liu, S. Wang, S. Tan, Q. Yu, Investigation of the effects of graphene and graphene oxide nanoplatelets on the micro- and macro-properties of cementitious materials, Constr. Build. Mater. 106 (2016) 102–114, https://doi.org/10.1016/j.conbuildmat.2015.12.092.
[42] S. Gupta, H.W. Kua, C.Y. Low, Use of biochar as carbon sequestering additive in cement mortar, Cem. Concr. Compos. 87 (2018) 110–129, https://doi.org/10.1016/j.cemconcomp.2017.12.009.
[43] K. Ogi, T. Shinoda, M. Mizui, Strength in concrete reinforced with recycled CFRP pieces, Compos. Part A Appl. Sci. Manuf. 36 (2005) 893–902, https://doi.org/10.1016/j.compositesa.2004.12.009.
[44] S. Wen, D.D.L. Chung, Partial replacement of carbon fiber by carbon black in multifunctional cement–matrix composites, Carbon N. Y. 45 (2007) 505–513, https://doi.org/10.1016/j.carbon.2006.10.024.
[45] A. Belli, A. Mobili, T. Bellezze, F. Tittarelli, P. Cachim, Evaluating the self-sensing ability of cement mortars manufactured with graphene nanoplatelets, virgin or recycled carbon fibers through piezoresistivity tests, Sustain. 10 (2018), https://doi.org/10.3390/su10114013.
[46] P. Azarsa, R. Gupta, Electrical Resistivity of Concrete for Durability Evaluation: A Review, Adv. Mater. Sci. Eng. 2017 (2017), https://doi.org/10.1155/2017/8453095.
[47] M. Chiarello, R. Zinno, Electrical conductivity of self-monitoring CFRC, Cem. Concr. Compos. 4 (2005) 463–469, https://doi.org/10.1016/J.CEMCONCOMP.2004.09.001.
[48] F. Javier Baeza, D.D.L. Chung, E. Zornoza, L.G. Andión, P. Garcés, Triple percolation in concrete reinforced with carbon fiber, ACI Mater. J. 107 (2010) 396–402, https://doi.org/10.14359/51663866.
[49] S. Jung, Y.K. Park, E.E. Kwon, Strategic use of biochar for CO2 capture and sequestration, J. CO2 Util. 32 (2019) 128–139, https://doi.org/10.1016/j.jcou.2019.04.012.
[50] D. Matovic, Biochar as a viable carbon sequestration option: Global and Canadian perspective, Energy. 36 (2011) 2011–2016, https://doi.org/10.1016/j.energy.2010.09.031.
[51] A.V. Saetta, B.A. Schrefler, R.V. Vitaliani, The carbonation of concrete and the mechanism of moisture, heat and carbon dioxide flow through porous materials, Cem. Concr. Res. 23 (1993) 761–772, https://doi.org/10.1016/0008-8846(93)90030-D.
[52] X. Dérobert, J.F. Lataste, J.P. Balayssac, S. Laurens, Evaluation of chloride contamination in concrete using electromagnetic non-destructive testing methods, NDT E Int. 89 (2017) 19–29, https://doi.org/10.1016/j.ndteint.2017.03.006.
[53] S. Gupta, H.W. Kua, S.D. Pang, Biochar-mortar composite: Manufacturing, evaluation of physical properties and economic viability, Constr. Build. Mater. 167 (2018) 874–889, https://doi.org/10.1016/j.conbuildmat.2018.02.104.
[54] Y. Liu, F. Presuel, Normalization of Temperature Effect on Concrete Resistivity by Method Using Arrhenius Law, Aci Mater. J. 111 (2014) 433–442, https://doi.org/10.14359/51686725.
[55] A. Çay, J. Yanık, Ç. Akduman, G. Duman, H. Ertaş, Application of textile waste derived biochars onto cotton fabric for improved performance and functional properties, J. Clean. Prod. 251 (2020), 119664, https://doi.org/10.1016/j.jclepro.2019.119664.
[56] O. Sengul, O.E. Gjørv, Effect of embedded steel on electrical resistivity measurements on concrete structures, ACI Mater. J. 106 (2009) 11–18, https://doi.org/10.14359/56311.